How to accurately monitor the weld penetration from dynamic weld pool serial images using CNN-LSTM deep learning model?

Rui Yu, Joseph Kershaw, Peng Wang, Member, IEEE, and YuMing Zhang*, Senior Member, IEEE

Abstract - This paper illustrates how a challenging problem be solved by assuring the adequacy of the raw information and using an appropriate deep learning network to extract the relevant information. The problem concerned is accurate monitoring of the penetration, in a fully penetrated weld pool, as quantified by the width of the weld on the back-side of the workpiece. This is challenging as the penetration occurs below the workpiece surface and is not visible. A popular method is to use a weld pool image to derive it. Analysis of the physical process suggests that a single weld pool does not contain adequate information but most recent serial weld pools may. As such, although a deep learning model may extract information that is already there, the raw information may not be sufficient. Hence, a model that is capable of extracting information from dynamic serial weld pool images is needed. To this end, a CNN-LSTM (convolutional neural network combined with long-short term memory one) model is proposed. Dynamic weld pools are experimentally generated using changing the welding current and welding speed randomly. The weld pools are imaged using an HDR camera during experiments. Images are also captured from the back-side surface of the workpiece to provide the ground truth for training, validation, and testing. It is found that the highly dynamically changing weld pool can be accurately predicted using serial weld pool images at 0.3 mm for its backside bead width. Comparison has been made with results from comparative studies to verify the effectiveness of and the contribution from the information adequacy (by using serial images) and the feature extracting capability (by using deep

Keywords: weld, weld penetration, deep earning, CNN, LSTM, CNN-LSTM, HDR image

I. INTRODUCTION

This work aims at precision monitoring of the weld penetration needed for its feedback control. Welding joins two workpieces together by melting their facing interfaces, and weld penetration quantifying the degree of such melting determines the integrity of the produced weld [1]. While the actual way to quantify varies with the application as detailed in [1], it is in common that such melting always occurs underneath the workpieces and is not directly visible [2], [3], in particular by a sensor attached to a welding torch operated by a moving robot/manipulator. The problem is thus challenging as it can only be estimated from indirect observables while they must contain adequate information about what occurs underneath. A further challenge is to effectively derive the penetration from the observables that are likely to be complex, as determined by the complex

welding phenomena, containing redundant information. The challenges increase further when the welding parameters are subject to dynamic adjustments so that the process is in continuous dynamic evolution. In such a case, the welding process phenomena become more complex and so does an effective derivation from the more complex observables. Unfortunately, such adjustments are fundamental for the monitoring to be used to provide the feedback for real-time control as being aimed in this study.

Weld pool formed by the melted metal is where complex welding process phenomena originate containing most of the raw information related to the degree of the melting, i.e., the state of the weld penetration [4]. Kotecki and Richardson made initial efforts [5] by correlating the weld pool oscillation frequency with its mass as a larger pool with greater mass/inertia oscillating slower. One major issue is that the weld pool is a 3D free liquid body and its mass is determined by 3D geometry while the penetration concerned is most correlated to its geometry in the depth direction. Xiao and de Ouden added a milestone by finding a large difference in the oscillation frequency among incomplete (partial) and complete (full) penetration [6], [7]: the frequency drastically reduces when the workpiece is fully melted/penetrated in its thickness direction. Developing from partial to full penetration changes the support to the weld pool bottom surface from un-melted solid metal to the gaseous ambiance so that the oscillation damping is drastically reduced. While this is effective in detecting the penetration mode (partial or full) in a stationary pool without a motion of the welding torch, it does not provide an accurate measure for the degree of the partial or full penetration and faces challenges in a moving pool where the pool shape becomes more complex. Various efforts have been made to improve the method over time [8], [9]. Other approaches have also been proposed including using ultrasound sensors [10], [11], infrared cameras [12], etc., and their principles and facing challenges are analyzed in [1].

Skilled welders can assure weld penetration by adjusting the welding parameters through their adaptive operation per their close observation on the weld pool. While the aforementioned approaches use specific information in the weld pool, for example, the temperature distribution from an infrared camera [12], it is hard to tell by the welders what specific information they pay attention to. Efforts have been

Rui Yu, Joseph Kershaw, Peng Wang and YuMing Zhang are with Institute for Sustainable Manufacturing and Department of Electrical and Computer Engineering, University of Kentucky, Lexington, KY 40506.

(corresponding

author: phone: 859-323-3262; e-mail: yuming.zhang@uky.edu).

focused on clearly imaging the weld pool [13]–[16] and effectively extracting the information from the weld pool images as observables contain welding phenomena in complex ways. Intuitive approaches are to measure the weld pool width and length. More advanced ways are to characterize/model the weld pool to introduce less intuitive but more abstract characteristic parameters [15], [17]. However, this is a hand-crafted engineering approach. As the phenomena are complex, effective extraction of the adequate characteristic parameter is challenging.

Deep learning can potentially provide an effective approach to extracting the state of the weld penetration from weld pool images similarly to a human welder. As such, CNNs have been used as a major type of deep learning model to extract relevant features automatically from weld pool images to predict the weld penetration through training from experimental data [18]–[22]. However, most studies are experimental and mathematical ignoring the basic physical ground if the weld pool images contain adequate raw information.

Weld pool images are taken from the workpiece surface. However, the weld pool itself is in 3D and the penetration is determined by its bottom underneath the workpiece. A question thus arises if one image from the visible weld pol surface contains sufficient raw information to tell what occurs underneath. As analyzed in Section II, this is unlikely to be true when the weld pool is in dynamic evolution and sequential weld pool images may be needed.

This study attempts to more accurately predict the backside width of the weld bead, which quantifies the state of the full penetration, using sequential images of a dynamically changing weld pool. To this end, we propose a CNN-LSTM model structure that complements CNN's capability for single image processing with that from the LSTM for counterparting the dynamic evolution. The paper is organized as follows: Section II discusses the physical process to justify why dynamic image series is needed while an overview of the collection of the raw data is given in Section III; Section IV details the neural network structure. Its training, validation, and testing are presented in Section V which also includes Discussion and Analysis. Finally, conclusions are drawn in Section VI.

II. BACKGROUND AND ANALYSIS

Fig. 1 shows the gas tungsten arc welding (GTAW) process. This is the most widely used process for the precision joining as it can provide the welding current, thus the arc power and arc heat, precisely, while another most widely used welding process gas metal arc welding (GMAW) cannot [18]. It also illustrates a completely penetrated weld pool whose state can be represented as the backside width w_b and height h_b of the liquid pool.

The most critical state is w_b . First, $w_b > 0$ is required as $w_b = 0$ means partial penetration that would cause an explosion under high temperature and pressure. Further, as the seam tracking error $e \ge 0$, the absolute deviation of the

weld symmetrical axis for the weld cross section (z in Fig. 1(b)) from the interface of the metals being joined (dot line in Fig. 1(b)), may not be avoidable, $w_b/2 < e$ will also cause the interface not be fully melted so that the penetration is actually also incomplete/partial.

To assure the required complete/full penetration, the desired w_b , denotated as w_b^* , needs to be appropriate. In general, a greater w_b^* better assures the required complete penetration; but as w_b increases, the heat input also increases causing greater distortion and residual stress, etc. w_b^* thus

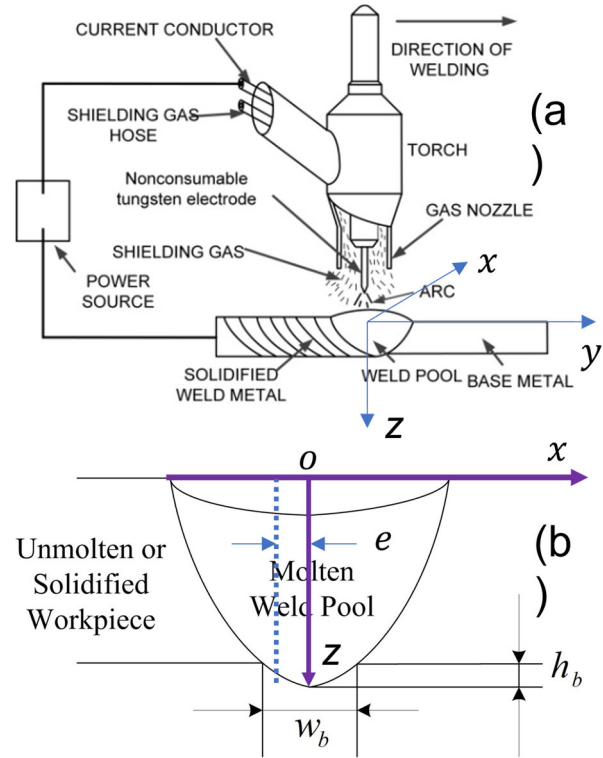


Fig.1 GTAW and complete weld penetration. (a) Illustration of GTAW process; (b) Cross section of the workpiece and weld. Axis z is that of the tungsten electrode and the weld is in general symmetrical about it. The dot-line in (b) is the interface of the two metals being joined and e is the seam tracking error.

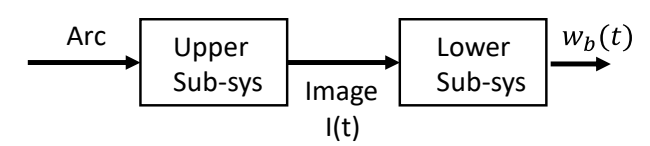


Fig.2 Dynamic development of the penetration.

should be minimized while assuring the complete penetration. Such minimization depends on the application, which determines the maximal weld seam tracking error e_{max} . This requires $2e_{max} \le w_b$ so that $2e_{max} \le w_b^*$. It also depends on the accuracy achievable for the monitoring and control of w_b . Denote ε as the estimation/control error between the estimated backside bead width \widehat{w}_b and actual one w_b so that $w_b = \widehat{w}_b + \varepsilon$. The condition $2e_{max} \le w_b$ thus becomes $2e_{max} + \varepsilon \le \widehat{w}_b$. Denoting, $\varepsilon_{max} \ge |\varepsilon|$ as the maximal estimation/control error, then $2e_{max} + \varepsilon_{max} \le w_b^*$. As can be seen, a precision monitoring, as well as a control, of the weld

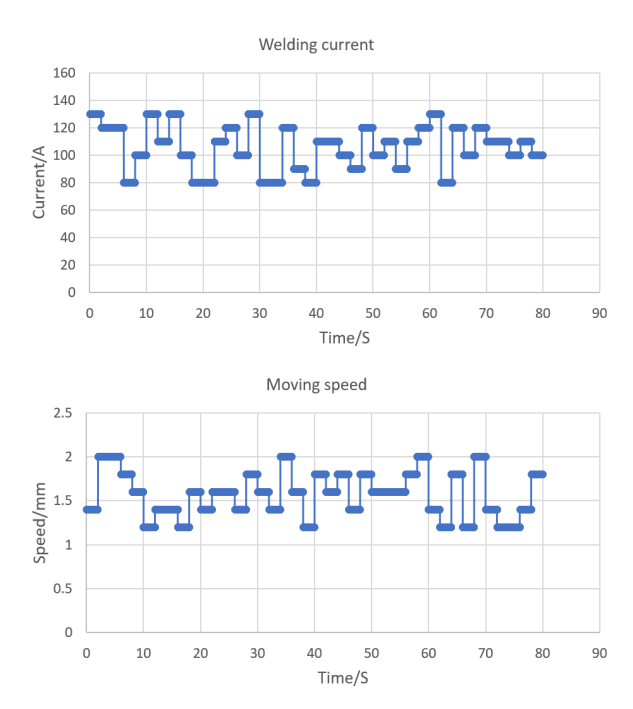


Fig.3 Welding current and travel speed in one experiment.

penetration is to minimize ε_{max} to minimize the heat input while assuring the complete penetration, i.e., fully melting of the interface along the entire thickness direction.

GTAW melts the workpiece in the following way: the arc heats the workpiece surface first; then the heat imposed on the surface is transferred in 3D in the workpiece including along the thickness direction to deepen the weld pool. One may artificially decompose this penetrating process into two subsystems (Fig. 2): upper subsystem and lower subsystem. The upper subsystem has the arc a(t) and upper weld pool (thus the image) I(t) as its input and output while the lower one has the upper weld pool as measured by I(t) and bottom surface as measured by $w_b(t)$ as its input and output. Because of the complex heat transfer and phenomena in the weld pool, $w_h(t) = f(I(\tau), \tau \le t)$. As such, using a single image I(t) to estimate $w_h(t)$ is only an approximation. The accuracy of such approximation largely depends on how significantly and how quickly $I(\tau)$ dynamically changes. Using $I(\tau)$, $t - \Delta t \le$ $\tau \le t$ with $\Delta t > 0$ provides more, and possibly the critical, raw information. An excessive Δt may not be necessary while increasing the computation and modeling complexity. We will correlate $I(\tau)$, $t - \Delta t \le \tau \le t$ to $w_b(t)$ using a CNN-LSTM network and compare its accuracy with a CNN that correlates just I(t) to $w_b(t)$. To this end, we will generate data pairs $(I(k), w_b(k))$]'s where k the discrete-time instant.

III. DATA GENERATION

A GTAW welding system at the University of Kentucky Welding Research Laboratory [23] has been used to perform GTAW welding experiments. During the experiment, one camera views the backside of the workpiece to capture the images $I_b(k)$ to be used to calculate $w_b(k)$ and a high dynamic range (HDR) camera views the weld pool to capture I(k). The images are synchronized in the recordings to form

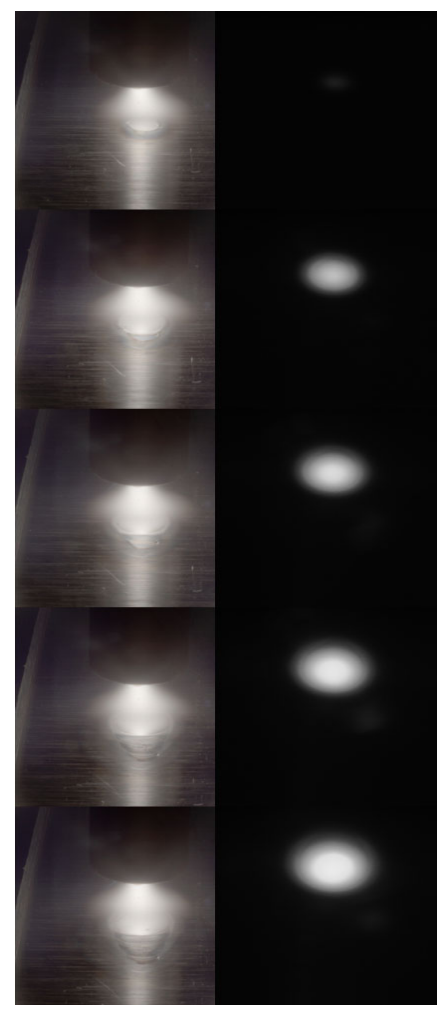


Fig.4 Example 5-second sequence of image pairs.

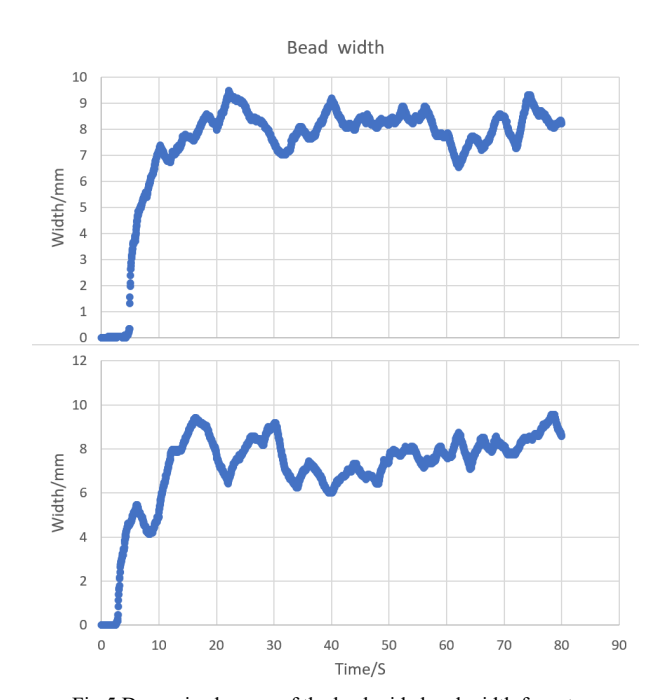


Fig.5 Dynamic changes of the back-side bead width from two experiments.

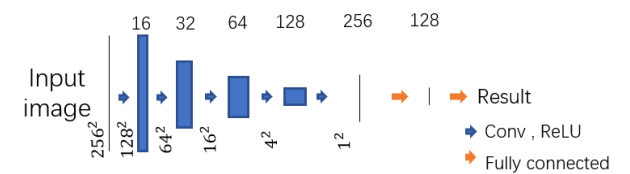


Fig.6 CNN architecture for comparative model.

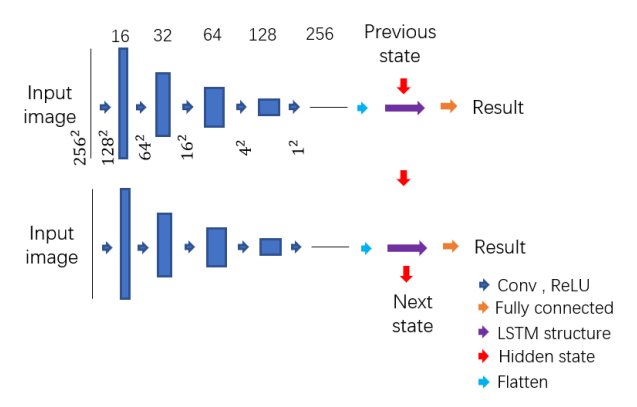


Fig.7 Proposed CNN-LSTM model structure.

 $(I(k), I_b(k))$ pairs. Cameras and welding torch are fixed while the workpiece is moved by a linear motion system. The welding current and travel speed vary every 2 seconds, within [80A, 130A] and [1.4 mm/s, 2.0mm/s], randomly to provide moving arc on 1.8 mm thick stainless steel. The current i and travel speed v together determine the heat input H, i.e., the input imposed on the workpiece in a unit length of weld: iv_{anode}/v where v_{anode} is the voltage on the workpiece which is the anode of the arc in GTAW. v_{anode} is considered a constant, when the shield gas and workpiece material are given, not changing with the welding current. While the heat input H is a major parameter in determining the penetration, the current i is also important as the arc pressure that largely controls the weld pool liquid metal flow thus the heat transfer within the pool is proportional to I^2 where I is the current.

Varying the current and travel speed is to generate dynamic evolution in the weld pool and this is needed as at least one of them will be adaptively adjusted if the weld penetration is not at the desired value. If the current and travel speed remain constant, the weld pool will be at a steady-state most of the time. The effect of I(m < k) on $w_h(k)$ will be unable or difficult to be observed. In this work, 6 experiments have been conducted and each experiment runs for 80 seconds approximately. Fig. 3 shows the current and travel speed in one experiment. Those in other experiments are similar but not exactly the same as they are different realizations of the same random processes. Fig. 4 provides a series of (I(k), $I_h(k)$)s in five seconds from the 60 frames/s recordings, with one second apart from each other. Each image I_h is binarized using to segment the image into bright and back regions and the width of the bright region is calculated as w_b [20] using a threshold. The threshold and the resolution mm/pixel are calibrated. As images were sampled at 60 Hz, 28,560 (I(k), $w_b(k)$) pairs are obtained. Fig. 5 shows w_b from two experiments to illustrate the dynamic changes.

IV. NETWORK MODEL

The comparative CNN's architecture is illustrated in Fig.6, which predicts $w_b(k)$ from a single image I(k). The proposed CNN-LSTM, which predicts from serial images I(m) ($m \le k$) is given in Fig. 7. Their CNNs are identical in structure and parameters are to be trained. Each image, all 256×256 , is fed into the CNN through its typical convolution layer followed by a pooling layer. This is repeated 4 times, with the parameters of convolution layers to be (1, 32, 5, 2, 2), (32, 64, 3, 2, 1), (64, 128, 3, 2, 1), (128, 256, 3, 2, 1) respectively. Batch normalization and ReLU activation were conducted between each convolution and pooling layer. After this convolution process, the input image is converted into a 1×256 feature vector V(k) to the input of the following fully connected layer to $w_b(k)$.

LSTM as a unique artificial recurrent neural network (RNN) architecture [24] with feedback connections can generate outputs from serial data. LSTM has outperformed other popular conventional dynamic prediction approaches like hidden Markov models in many tests [25]. As such, it is natural to hypothesize that incorporating LSTM with CNN may provide an effective approach to automatically extract relevant dynamic and abstract features from serial dynamic weld pool images to predict the weld penetration occurring underneath the workpiece.

In the proposed CNN-LSTM model shown in Fig. 7, V(k) is connected to the LSTM model rather than the fully connected layer. The size of the input V of the LSTM model is thus 256. In our study, we first try 128 for the hidden size, 3 for the num_layers set, and 8 for the sequence length to see if we can obtain desirable results. Because the hidden state in the RNN will receive the previous state information, the previous state will then be able to influence the current state, which means that our earlier images I(m < k) will also make a contribution to help predict current $w_b(k)$.

We captured images at 60 frames per second and set the batch size as 32. Each batch thus took 1.875 images per second. With the sequence length of 8, the model will use V as far as 4 seconds ago. As such, the CNN-LSTM uses $V(k-j)(j \le 32 * 7 = 224$, i.e., image series I(k), I(k-33), ..., I(k-224) to predict $w_b(k)$. 4 seconds reflect the settling time approximately of the GTAW process which was illustrated in Fig. 9 in ref [26].

V.TRAINING, RESULTS, AND DISCUSSION

We perform the training, validation, and testing process on a NVIDIA GTX 2080 graphic card. Both models were trained iteratively 100 times with SGD optimizer and mean-square loss under Python environment with Pytorch library.

Of the data from six experiments, those from four of them were used for training and from other two were used for validation and test respectively. Each experiment was performed under the same nominal welding conditions; however, as the welding parameters changed randomly, each experiment is different from other experiments in a random way. Hence, there is no need for random selection at the data level and any experiment can serve for training, validation, or testing.

The 28,560 paired images in our dataset were thus used to form three subsets: training, validation, and testing. The sizes are 19040, 4760 and 4760, respectively. To train the CNN model, the dataset has been shuffled to make sure the data has been drawn randomly. For training the CNN-LSTM model, the data was pre-arranged: divided as multiple sequences with each containing 8 images and the difference between the frame number was 32, for example, one sequence would contain frame 1, frame 33, frame 65, etc. In this way, we could ensure that the images fed into the CNN-LSTM model have the time correlation with each other and each frame follows the previous frame in the sequence after 0.53s.

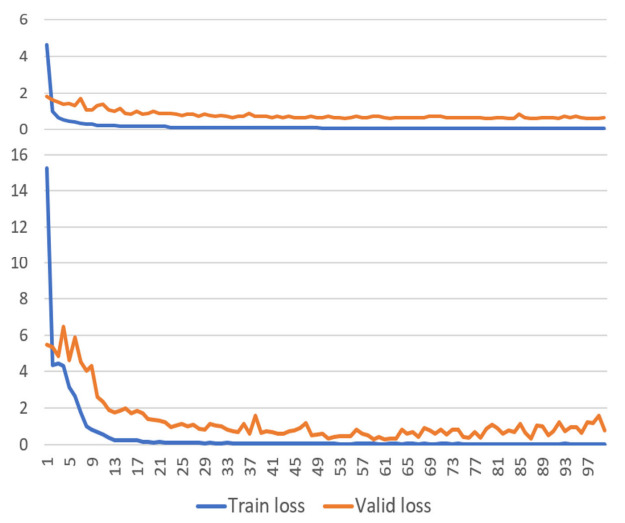


Fig.8 CNN training curve (Top) and CNN-LSTM training curve (Bottom).

The results of loss in training and validation datasets for both networks are presented in Fig. 8. It is obvious that with the mean square error loss (MSE), the model which adds the

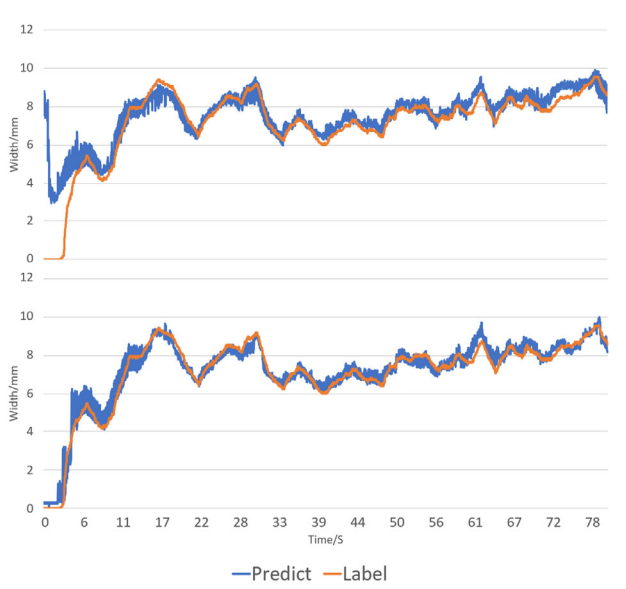


Fig.9 CNN (Top) and CNN-LSTM (Bottom) performance on test data.

LSTM could reduce the validation error much further than the CNN model without LSTM. In particular, while the CNN

realized the minimal validation error of $0.6mm^2$, CNN-LSTM achieved at $0.34mm^2$, realizing 43 percent of reduction. It is critical for accurate monitoring for the precision joining this work targets.

The network has been trained with the mean squared error as the loss. An absolute error-based loss is logically more reasonable. However, mean squared error-based losses have analytical gradients helping lead to more efficient solutions. In addition, absolute error-based losses minimize the mean of the absolute error and such mean is still not the maximal absolute error ε_{max} . Hence, for the present paper that contributes by proposing dynamic image series through analysis of physical process to assure the adequacy of the raw information, the use of the particular network, loss, and learning algorithm should not affect the objective for verification of the idea using dynamic images to assure the adequacy in the raw information.

Both models were selected at the above epochs of their respective minimum validation error to test. Fig. 9 illustrates the prediction results for the test experiment. The average error was 0.54 mm for the CNN model while it was 0.3 mm for the CNN-LSTM model. This reflects a 44 percent reduction in the prediction error and this is simply contributed by adding LSTM to the CNN.

In particular, as can be seen, the CNN model performed particularly less ideal in the beginning of the welding during which the weld pool is most dynamic. The CNN-LSTM model performed fundamentally differently, having successfully tracked the fast rise of the weld penetration. To our knowledge, this is extremely challenging and only few efforts have been reported to predict the weld penetration under such a drastic dynamic change. In addition, in the entire range of the experiment where the dynamics demonstrated different randomness, the CNN-LSTM model achieved outstanding performance. The achieved 0.3 mm error is ultraaccurate for the welding process that applies an arc with a broad arc heat distribution and there are many factors affecting the transfer of the heat to the bottom of the workpiece.

We have not been successful in finding many reports, that plot a curve as in Fig. 9 to directly compare the actual and predicted weld penetration using a deep learning approach, to compare with our results. Fig. 10 shows the result from a previous effort using a CNN model to estimate the growth of the weld penetration for a stationary weld pool without a relative motion between the arc and workpiece. Fig. 11 shows the results from previous efforts using hand-crafted features from moving weld pool. In (a), the 3D surface of the weld pool was measured using an innovative approach by projecting a laser dot-matrix to this mirror-like specular surface and intercepting the reflected laser rays [27]. The 3D surface was characterized by the length and width of the weld pool together with a proposed novel key parameter "convexity" of the irregular 3D weld pool surface [28]. (a) compares the actual and 3D weld pool surface characteristic parameters predicted weld penetration. In (b), a series of weld pool images were used as the input to estimate the back-side width of the weld. However, the weld pool images are not

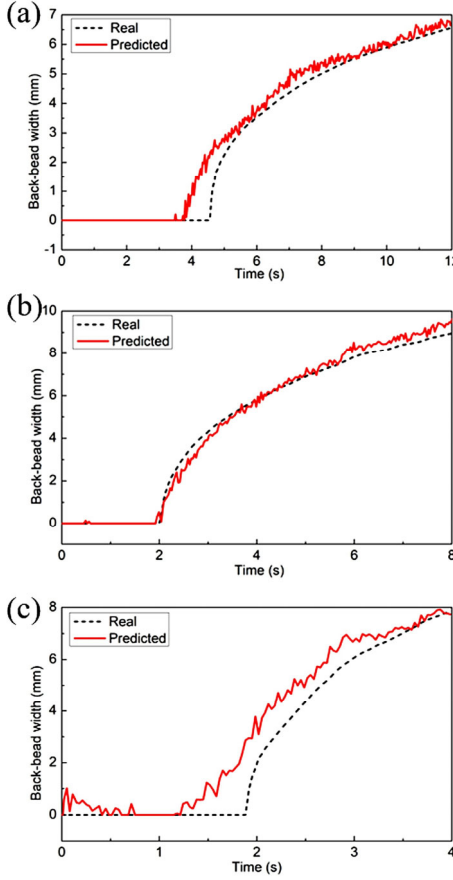
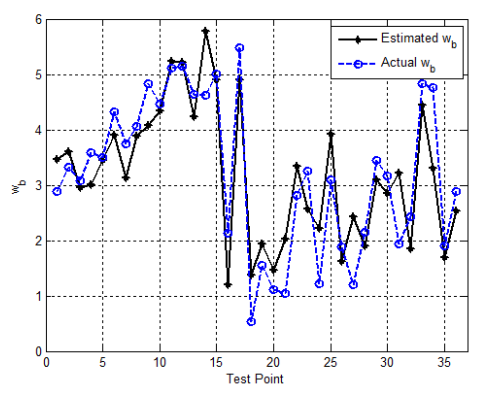


Fig. 10 Comparative efforts in predicting the weld penetration at different welding current using CNN [20]. (a) 60 A; (b) 83 A; (c) 110 A.

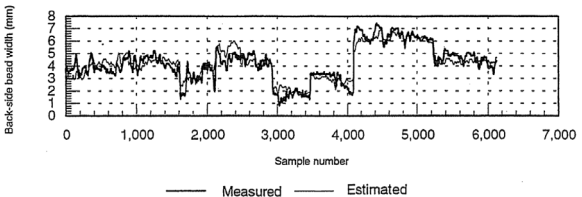
directly used to automatically extract the abstract features as in deep learning. Instead, hand-drafted features were proposed to represent the weld pool boundary. The resultant features in the most recent 5 seconds were used to estimate the back-side weld width using a neural network. As can be seen, their accuracies are far below that achieved in this work. In particular, (a) demonstrated that a single image, even if from an accurate 3D surface, is not sufficient; and (b) illustrated that manual hand-craft is difficult to extract the right information. As such, deep-learning that may automatically extract the right information and serial images that contain adequate information are both critical and CNN-LSTM is their mathematical surrogate.

VI. CONCLUSION AND FUTURE WORK

This work used randomly varying waveforms for the welding current and travel speed to generate dynamic weld pools. It found that serial weld pool images in the most recent 5 seconds contain adequate raw information to estimate the back-side bead, which quantifies the degree of the full penetration. However, a single weld pool image acquired at the current time does not in particular when the weld pool experiences a rapid dynamic evolution. A CNN-LSTM is capable of extracting the relevant dynamic features from the serial images to determine a rapidly changing weld penetration accurately. The effect and the contribution from the CNN-based deep learning model and the serial images are



 (a) Prediction using 3D weld pool surface as characterized by width, length, and convexity of the liquid weld pool surface [27]



b) Prediction using dynamic 2D weld pool boundaries as input of a neural network [2]

Fig. 11 Comparative efforts in predicting the weld penetration using hand-crafted features.

separately verified through comparative studies. The resultant CNN-LSMT model can estimate the back-side weld bead at 0.3 mm accuracy from the serial weld pool images captured by an HDR camera despite random changes in the major welding parameters.

While using weld pool images and deep learning networks has become a popular and standard approach to monitor the weld penetration in recent literature, there has a critical lack on analyzing the adequacy of the raw information used. This paper analyzed the dynamic weld pool evolution that determines the weld penetration. Per the analysis, the weld pool images must be serial in order to for the raw information to be adequate to reflect the critical dynamic evolution. This provides a novel innovative thinking and direction to choose the raw information and design the needed models accordingly. It played a decisive role in improving the prediction accuracy when the weld pool is under dynamic adjustment/development as in the beginning of the welding.

Specially, in order to represent the dynamic changes of the weld penetration process, we need weld pool images in most recent 4 second period to reflect the settling time for the GTAW process. We also picked one image from every 2^5=32 images captured at 60 Hz, resulting in 0.53 second sampling time, as if the sample time is lower the secretive images would hardly demonstrate differences. Furthermore, using less number of images helps control the network to an manageable size. We found most recent 8 images contain adequate features needed to predict the backside bead width. Our innovative, analysis-based network structure design thus contributed to solving the weld pool images-based weld

penetration prediction problem for the GTAW that is the most widely used welding process for critical applications where the weld penetration must be assured.

The effectiveness of the prediction under dynamic adjustment/development of the weld pool is crucial for real-time control of the weld penetration. We expect that the proposed method will be particularly useful when applied to real-time control where the weld pool is subject to continuous dynamic adjustment. We will apply the proposed method to obtain the feedback for real-time control of weld penetration and compare its accuracy in resultant welds with using feedback from non-serial images-based models.

ACKNOWLEDGMENT

This study is supported by National Science Foundation under Grant No. 2024614.

REFERENCES

- [1] Y. ZHANG, Q. WANG, and Y. LIU, "Adaptive Intelligent Welding Manufacturing," *Welding Journal*, vol. 100, no. 01, pp. 63–83, Jan. 2021, doi: 10.29391/2021.100.006.
- [2] Y. M. Zhang, L. Li, and R. Kovacevic, "Dynamic Estimation of Full Penetration Using Geometry of Adjacent Weld Pools," *Journal of Manufacturing Science and Engineering*, vol. 119, no. 4A, pp. 631–643, Nov. 1997, doi: 10.1115/1.2831197.
- [3] Y. Cheng, R. Yu, Q. Zhou, H. Chen, W. Yuan, and Y. M. Zhang, "Real-time sensing of gas metal arc welding process – A literature review and analysis," *Journal of Manufacturing Processes*, vol. 70, pp. 452–469, Oct. 2021, doi: 10.1016/J.JMAPRO.2021.08.058.
- [4] Y. M. Zhang, Y. P. Yang, W. Zhang, and S. J. Na, "Advanced Welding Manufacturing: A Brief Analysis and Review of Challenges and Solutions," *Journal of Manufacturing Science and Engineering, Transactions of the ASME*, vol. 142, no. 11, Nov. 2020, doi: 10.1115/1.4047947/1085926.
- [5] D. J. Kotecki, D. L. Cheever, and D. G. Howden, "Mechanism of Ripple Formation During Weld Solidification Ripples on GTA spot welds are explained by pool sur-face oscillations during solidification, as seen by high speed motion pictures".
- [6] Y. H. Xiao and G. den Ouden, "Weld Pool Oscillation during GTA Welding of Mild Steel The oscillation behavior of the GTA weld pool depends on the welding conditions and can be used for in-process control of weld penetration".
- [7] Y. H. Xiao and G. den Ouden, "A Study of GTA Weld Pool Oscillation Monitoring oscillation frequency in the weld pool may offer a means of controlling joint penetration".
- [8] M. Sommer, J.-P. Weberpals, S. Müller, P. Berger, and T. Graf, "Advantages of laser beam oscillation for remote welding of aluminum closely above the deep-penetration welding threshold," *Journal of Laser Applications*, vol. 29, no. 1, p. 012001, Nov. 2016, doi: 10.2351/1.4963399.
- [9] H. Maruo and Y. Hirata, "Natural frequency and oscillation modes of weld pools. 1st Report: Weld pool oscillation in full penetration welding of thin plate," http://dx.doi.org/10.1080/09507119309548457, vol. 7, no. 8, pp. 614–619, Jan. 2009, doi: 10.1080/09507119309548457.
- [10] R. FENN, "ULTRASONIC MONITORING AND CONTROL DURING ARC FUSION WELDING," http://dx.doi.org/10.1080/10589758508952913, vol. 2, no. 2, pp. 43–53, Jun. 2007, doi: 10.1080/10589758508952913.
- [11] L. A. Lott, J. A. Johnson, and H. B. Smartt, "Real-time ultrasonic sensing of arc welding processes," Jan. 1983, doi: 10.2172/6810314.

- [12] K. Yamazaki et al., "Measurement of surface temperature of weld pools by infrared two colour pyrometry," Science and Technology of Welding and Joining, vol. 15, no. 1, pp. 40–47, Jan. 2010, doi: 10.1179/136217109X12537145658814.
- [13] B. Zhang, Y. Shi, Y. Cui, Z. Wang, and X. Chen, "A high-dynamic-range visual sensing method for feature extraction of welding pool based on adaptive image fusion," *International Journal of Advanced Manufacturing Technology*, vol. 117, no. 5–6, pp. 1675–1687, Nov. 2021, doi: 10.1007/S00170-021-07812-X.
- [14] R. Yu, J. Kershaw, P. Wang, and Y. M. Zhang, "Real-time recognition of arc weld pool using image segmentation network," *Journal of Manufacturing Processes*, vol. 72, pp. 159–167, Dec. 2021, doi: 10.1016/J.JMAPRO.2021.10.019.
- [15] J. S. Chen, J. Chen, K. Zhang, Z. Feng, and Y. M. Zhang, "Dynamic reflection behaviors of weld pool surface in pulsed GTAW," *Welding Journal*, vol. 97, no. 6, pp. 191s–206s, Jun. 2018, doi: 10.29391/2018.97.017.
- [16] "Gas Metal Arc Weld Pool Surface Imaging: Modeling and Processing-Web of Science Core Collection." https://www-webofscience-com.ezproxy.uky.edu/wos/woscc/full-record/WOS:000290083700020 (accessed Feb. 22, 2022).
- [17] Y. K. Liu and Y. M. Zhang, "Model-Based predictive control of weld penetration in gas tungsten arc welding," *IEEE Transactions* on Control Systems Technology, vol. 22, no. 3, pp. 955–966, 2014, doi: 10.1109/TCST.2013.2266662.
- [18] W. Jiao, Q. Wang, Y. Cheng, and Y. M. Zhang, "End-to-end prediction of weld penetration: A deep learning and transfer learning based method," *Journal of Manufacturing Processes*, vol. 63, pp. 191–197, Mar. 2021, doi: 10.1016/J.JMAPRO.2020.01.044.
- [19] J. Kershaw, R. Yu, Y. M. Zhang, and P. Wang, "Hybrid machine learning-enabled adaptive welding speed control," *Journal of Manufacturing Processes*, vol. 71, pp. 374–383, Nov. 2021, doi: 10.1016/J.JMAPRO.2021.09.023.
- [20] Q. Wang, W. Jiao, P. Wang, and Y. M. Zhang, "A tutorial on deep learning-based data analytics in manufacturing through a welding case study," *Journal of Manufacturing Processes*, vol. 63, pp. 2–13, Mar. 2021, doi: 10.1016/J.JMAPRO.2020.04.044.
- [21] W. JIAO, Q. WANG, Y. CHENG, R. YU, and Y. ZHANG, "Prediction of Weld Penetration Using Dynamic Weld Pool Arc Images," *Welding Journal*, vol. 99, no. 11, pp. 295s–302s, Nov. 2020, doi: 10.29391/2020.99.027.
- [22] C. LI, Q. WANG, W. JIAO, M. JOHNSON, and Y. M. ZHANG, "Deep Learning-Based Detection of Penetration from Weld Pool Reflection Images," *Welding Journal*, vol. 99, no. 9, pp. 239s– 245s, Sep. 2020, doi: 10.29391/2020.99.022.
- [23] Y. Cheng et al., "Detecting dynamic development of weld pool using machine learning from innovative composite images for adaptive welding," *Journal of Manufacturing Processes*, vol. 56, pp. 908–915, Aug. 2020, doi: 10.1016/J.JMAPRO.2020.04.059.
- [24] S. Hochreiter and J. Schmidhuber, "Long Short-Term Memory," Neural Computation, vol. 9, no. 8, pp. 1735–1780, Nov. 1997, doi: 10.1162/NECO.1997.9.8.1735.
- [25] A. Sherstinsky, "Fundamentals of Recurrent Neural Network (RNN) and Long Short-Term Memory (LSTM) Network," *Physica D: Nonlinear Phenomena*, vol. 404, Aug. 2018, doi: 10.1016/j.physd.2019.132306.
- [26] Y. M. Zhang and R. Kovacevic, "Neurofuzzy model-based predictive control of weld fusion zone geometry," *IEEE Transactions on Fuzzy Systems*, vol. 6, no. 3, pp. 389–401, 1998, doi: 10.1109/91.705507.
- [27] "(PDF) Characterization of Three-dimensional Weld Pool Surface in Gas Tungsten Arc Welding."
 https://www.researchgate.net/publication/260986477_Characteriz ation_of_Three-dimensional_Weld_Pool_Surface_in_Gas_Tungsten_Arc_Weldin g (accessed Feb. 26, 2022).
- [28] J. S. Chen, J. Chen, K. Zhang, Z. Feng, and Y. M. Zhang, "Dynamic Reflection Behaviors of Weld Pool Surface in Pulsed GTAW," Welding Journal, vol. 97, no. 6, pp. 191s–206s, Jun. 2018, doi: 10.29391/2018.97.017.